DOI: 10.1002/anie.200900117

Single-Molecule Magnets

Iron Polyoxometalate Single-Molecule Magnets**

Jean-Daniel Compain, Pierre Mialane, Anne Dolbecq, Israël Martyr Mbomekallé, Jérôme Marrot, Francis Sécheresse, Eric Rivière, Guillaume Rogez, and Wolfgang Wernsdorfer*

Dedicated to Professor Gilbert Hervé on the occasion of his retirement

Single-molecule magnets (SMMs) are molecules that can be magnetized in a magnetic field and which, at very low temperatures, retain the magnetization when the external field is switched off.[1] They exhibit hysteresis loops in magnetization versus field experiments. The key requirement for such behavior is the presence of Ising-type anisotropy (easy axis of magnetization) together with a relatively large magnetic moment, leading to an energy barrier to the relaxation of the magnetization. The height of the barrier U characterizing each member of this family of compounds is governed by the value of the spin ground state S (assuming that this state is well-separated from the excited states) and the magnitude of the Ising-type anisotropy (characterized by the axial zero-field splitting (ZFS) parameter D), with $U = |D|S^2$ for an integer spin and $U = |D|(S^2-1/4)$ for a half-integer spin. The spin reorientation can occur either by thermal processes or by quantum tunneling of magnetization (QTM).[2] To date, most of the characterized complexes exhibiting SMM behavior are high-nuclearity high-spin transition-metal clusters, but it has also been shown that mononuclear rare-earth compounds can behave as nanomagnets.[3] A vast majority of these species have been synthesized in the presence of organic ligands, and it is only recently that Cronin, Murrie, and co-workers reported the first 3d polyoxometalate (POM) compound exhibiting SMM behavior. In this compound, a mixed-valence $[Mn^{III}{}_4Mn^{II}{}_2O_4(H_2O)_4]^{8+}$ core is encapsulated between two $\{XW_9O_{34}\}$ ($X = Ge^{IV}, Si^{IV}$) moieties.[4] At the same time, an example of a POM lanthanide single-ion SMM was reported by Coronado, Gaita-Ariño, and co-workers.[5] The observation that POM ligands can be used for the synthesis of transition-metal-based SMMs is in line with the observation that polyoxotungstate ligands are able to induce very strong axial magnetic anisotropy, leading to the presence of an easy axis of magnetization.[6] But the implication of the POM compounds in the SMM field is limited by the fact that no magnetic polyoxotungstate characterized by a well-isolated spin ground state with an S value greater than 6[7] has been reported, despite the large number of high-nuclearity magnetic POM clusters reported to date.[8] From a synthetic point of view, the strategy considered to obtain such systems had mainly consisted in the combination of 3d cations with POM ligands characterized by the presence of diamagnetic heteroatoms and a large number of lacunary sites, as exemplified by the multinuclear species obtained using the trivacant $\{XW_9O_{34}\}$ systems ($X = P^V$,[9] Si^{IV},[10] …), the hexavacant $[H_2P_2W_{12}O_{48}]^{12-}$ entity,[11] or the crown-shaped ligand $[H_7P_8W_{48}O_{184}]^{33-}$.[12] In contrast, the synthesis of high-nuclearity POM complexes possessing magnetic heteroatoms remains largely unexplored. Indeed, to date, most of the POM compounds containing a paramagnetic heteroelement were saturated $\{XM_{12}O_{40}\}$[13] or monovacant $\{XM_{11}O_{39}\}$[14] ($X = Fe^{III}$, Cu^{II}, Co^{II}) Keggin-type complexes. Nevertheless, pentanuclear[15] and hexanuclear[16] sandwich-type species have also been reported, showing that systems containing multiple paramagnetic heteroatoms can also be obtained using this strategy. We have initiated a systematic study of the $WO_4{}^{2-}/M^{n+}$ system, where M^{n+} is a magnetic 3d transition-metal cation. Herein we report on nonairon(III) and hexairon(III) complexes that have been found to exhibit SMM behavior.

Hydrothermal reaction of tungstate, iron(III), and tetramethylammonium at pH 7 afforded a precipitate, which was filtered off. Slow evaporation of the filtrate yielded large orange crystals of $Na_{14}(C_4H_{12}N)_5[(Fe_4W_9O_{34}(H_2O))_2(FeW_6O_{26})]\cdot 50H_2O$ (**1**). Further evaporation of the supernatant after removal of **1** leads after several days to small yellow crystals of $Na_6(C_4H_{12}N)_4[Fe_4(H_2O)_2(FeW_9O_{34})_2]\cdot 45H_2O$ (**2**). The purity of each phase can be checked by comparison of the experimental X-ray powder diffraction pattern with the powder pattern calculated from the structure solved from single-crystal X-ray diffraction data (Figure SI1 in the Supporting Information). In **1**, the vacancies of two [B-α-$FeW_9O_{34}]^{11-}$ trivacant ligands (where B refers to the

[*] J.-D. Compain, Prof. P. Mialane, Dr. A. Dolbecq, Dr. I. M. Mbomekallé, Dr. J. Marrot, Prof. F. Sécheresse
Institut Lavoisier de Versailles, UMR 8180
Université de Versailles Saint-Quentin
45 Avenue des Etats-Unis, 78035 Versailles Cedex (France)
Fax: (+33) 1-3925-4381
E-mail: mialane@chimie.uvsq.fr
Dr. E. Rivière
Institut de Chimie Moléculaire et des Matériaux d'Orsay, UMR 8182
Equipe Chimie Inorganique, Université Paris-Sud
91405 Orsay Cedex (France)
Dr. G. Rogez
Institut de Physique et de Chimie des Matériaux de Strasbourg (IPCMS), UMR 7504 (CNRS Université de Strasbourg)
23 rue de Lœss, BP 43, 67034 Strasbourg Cedex 2 (France)
Dr. W. Wernsdorfer
Institut Néel, CNRS & Université J. Fourier
BP-166, Grenoble Cedex 9 (France)

[**] We thank Prof. T. Mallah for fruitful discussions. This work was supported by the CNRS, the Ministère de l'Enseignement Supérieur et de la Recherche and the ANR (06-JCJC-0146 and 08-NANO-P110-48).

Supporting information for this article is available on the WWW under http://dx.doi.org/10.1002/anie.200900117.

orientation of the $\{FeO_4\}$ tetrahedron) are filled by three Fe^{III} cations, forming two tetranuclear $\{Fe_4W_9\}$ subunits, which are connected by an $\{FeW_6O_{26}\}$ cluster (Figure 1 a). Valence-bond calculations[17] (Table SI1 in the Supporting Information)

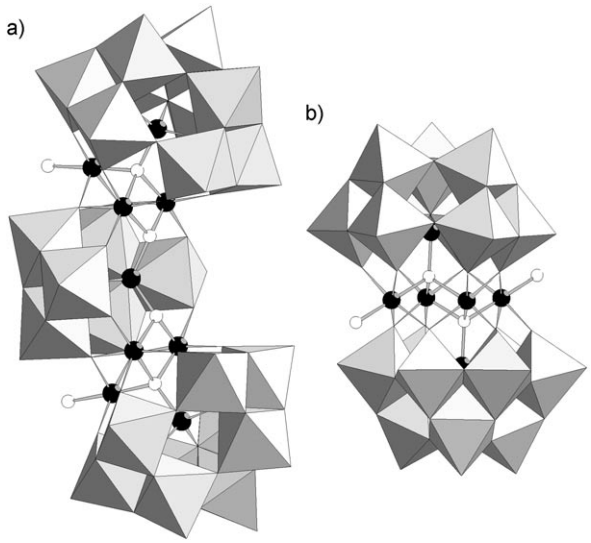

Figure 1. Mixed polyhedral and ball-and-stick representations of a) complex **1** and b) complex **2**. Gray octahedra WO_6, black spheres Fe, white spheres O.

indicate that in this nonairon cluster, all the iron centers are in the oxidation state +III and that two iron centers are coordinated to two terminal water molecules, while the other oxygen atoms in this POM are not protonated. Concerning the paramagnetic ions, the three Fe^{III} cations acting as heteroelements (noted Fe_{tet}) adopt a tetrahedral geometry, while the six remaining iron centers (noted Fe_{oct}) are in octahedral environments. This complex can be compared to the reported $[Ni_6As_3W_{24}O_{94}(H_2O)_2]^{17-}$ and $[Co_7(H_2O)_2(OH)_2P_2W_{25}O_{94}]^{16-}$ POMs,[18] with nine Fe^{III} ions in **1** replacing both the paramagnetic ions and the diamagnetic heteroatoms present in these two complexes. Compound **2** consists of two $[B\text{-}\alpha\text{-}FeW_9O_{34}]^{11-}$ trivacant units similar to those found in **1**, but in **2**, these two fragments sandwich a $\{Fe_4(H_2O)_2O_{14}\}$ tetranuclear cluster (Figure 1 b). This species is analogous to the hexanuclear alkali salt previously reported by Krebs and co-workers[16c] and to the peroxo compound recently reported by the group of Neumann.[19] It can also be compared to the hexanuclear mixed-valent compound $[Fe^{II}{}_2Fe^{II}{}_2(enH)_2(Fe^{III}W_9O_{34})_2]^{10-}$ (en = ethylenediamine), in which the Fe^{II} centers are stabilized by pendant en ligands.[16b]

UV/Vis spectroscopy (Figure SI2 in the Supporting Information) and electrochemical studies revealed that both **1** and **2** are stable in aqueous solution at pH 0–7 (see the Supporting Information). Figure 2 and Figure SI3 in the Supporting Information show the cyclic voltammograms of **1** and **2**, respectively, in 0.5 M aqueous Li_2SO_4 (pH 1). The main observation is the stepwise reduction of the Fe^{III} centers sandwiched between the tungsten skeletons $\{FeW_9\}$ and $\{FeW_6\}$, which can be compared to the reduction processes previously described for sandwich-type complexes containing

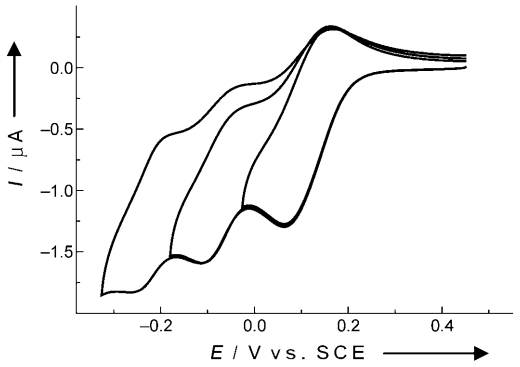

Figure 2. Cyclic voltammogram of **1** in a 0.5 M $Li_2SO_4 + H_2SO_4$ solution at pH 1. Working electrode: glassy carbon; reference electrode: saturated calomel electrode (SCE); scan rate: 10 $mV s^{-1}$; POM concentration: 0.14 mM.

iron(III).[20] Furthermore, the cyclic voltammograms and controlled-potential coulometry experiments confirm the electrochemical inertia of the Fe_{tet} heteroatoms. Among this family of POMs that contain a d metal as heteroatom, only the Co^{II} center encapsulated inside the $[CoW_{12}O_{40}]^{6-}$ derivative is known to be electroactive.[20c] Controlled-potential coulometry experiments were carried out at pH 5 to determine the total number of electrons involved in this process. The potential was set at −0.620 V versus SCE, yielding 6.02 ± 0.05 electrons per molecule of **1** and 3.98 ± 0.05 electrons per molecule of **2**. These results are consistent with the reduction of the six and four Fe^{III} centers in **1** and **2**, respectively. The characteristic blue color associated with a reduced tungsten–oxygen framework was not observed in either case during these experiments, a consequence of the relatively large potential gap between the Fe^{III}- and W^{VI}-based redox processes (Figure SI5 in the Supporting Information). Another important point is the determination of the number of electrons exchanged at each Fe^{III} reduction step. For the polyanion **2**, based on the peak reduction current, the three successive redox steps are two-, one-, and one-electron processes, respectively. The behavior of the six electroactive Fe^{III} centers in **1** is less classical. Controlled-potential coulometry experiments (with potential set at −0.160 V vs. SCE at pH 3) indicate that in **1** 2.92 ± 0.05 electrons per molecule are exchanged on the first wave, and then by comparison (based on their relative heights) that three, two, and one electron per molecule are exchanged on the first, second, and third waves, respectively. A quasi-nonreversible wave featuring the reduction of the tungsten framework follows the reduction of Fe^{III} centers for both compounds. This composite wave shifts towards negative potentials as the pH value of the electrolyte is increased (Table SI2 in the Supporting Information). This common behavior of POMs is related to the influence of protonation during the redox process.[20c]

The magnetic behavior of **1** was investigated in the 2–300 K temperature range. The $\chi_M T$ curve (χ_M is the molar magnetic susceptibility) exhibits a continuous increase when the temperature is decreased (Figure SI6 in the Supporting Information), but over the entire experimental temperature

range the value of $\chi_M T$ is lower than that calculated for nine isolated $S = 5/2$ centers ($\chi_M T = 39.375\ cm^3 mol^{-1} K$, assuming $g = 2$), indicating antiferromagnetic interactions. Considering that the determination of the magnetic exchange parameters by direct diagonalization of the adapted Heinsenberg–Dirac–Van Vleck Hamiltonian is not possible given the size of the matrices involved (ca. $10^7 \times 10^7$), we focused our study on the determination of the nature of the spin ground state. The curves $M = f(HT^{-1})$ at 2, 4, 6, and 8 K are shown in Figure 3.

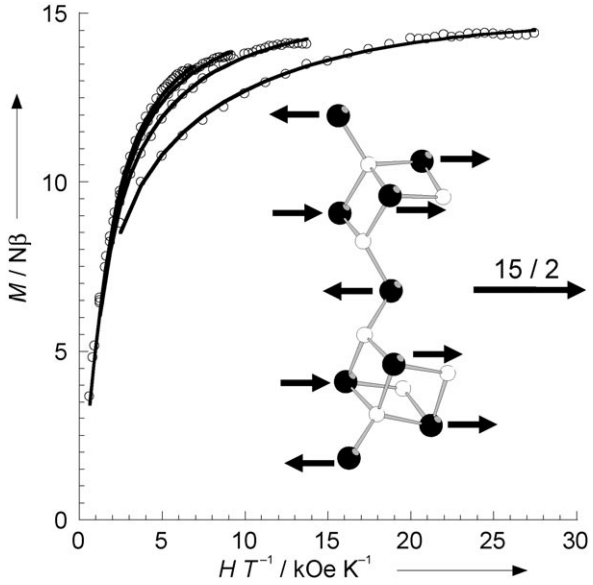

Figure 3. Magnetization versus magnetic field divided by temperature at 2, 4, 6, and 8 K (from right to left) for compound **1**. The solid lines were generated from the best-fit parameters given in the text. Inset: spin alignments in **1** of the $S = 5/2$ spins localized on the nine Fe^{III} centers, leading to the overall $S = 15/2$ ground state.

These curves saturate at a value close to $M = 15\,N\beta$, where N is Avogadro's number and β is the Bohr magneton, suggesting an $S = 15/2$ ground state. An excellent fit of these data considering the Hamiltonian in Equation (1):

$$\hat{H} = g\mu_B H\hat{S} + D\left[\hat{S}_z^2 - \frac{1}{3}S(S+1)\right] + E\left[\hat{S}_x^2 + \hat{S}_y^2\right] \quad (1)$$

with $g = 2.00$ afforded the parameters $S = 15/2$, $|D| = 0.24\ cm^{-1}$, and $|E/D| = 0.18$ ($R = 6.8 \times 10^{-5}$).[21] The multiplicity of the ground state can be rationalized in terms of magnetostructural correlations. First, it is well known that for oxo-bridged high-spin Fe^{III} compounds small Fe–O bond lengths d and large Fe-O-Fe angles θ lead to large antiferromagnetic interactions.[22] Second, it has been shown that the magnetic interactions through Fe-O(W)-Fe bridges are much weaker than those occurring through oxo ligands,[23] implying that in **1** the magnetic interactions involving the μ_3-oxo ligands are predominant. In **1**, all the Fe–O distances involving the Fe^{III} heteroatoms and bridging Fe-(μ_3-O)-Fe oxo ligands are in the 1.83–1.87 Å range (Fe_{tet}-(μ_3-O)-Fe_{oct} ca. 118°), while the corresponding Fe–O distances involving the Fe^{III} cations in octahedral environments are in the 1.97–2.08 Å range (Fe_{oct}-(μ_3-O)-Fe_{oct} ca. 100°). Considering these d and θ values, it follows that the exchange coupling involving the Fe_{tet} and Fe_{oct} centers is stronger than that involving only the Fe_{oct} cations. Thus, the Fe_{tet}–Fe_{oct} interactions will dominate, leading to the spin topology depicted in the inset of Figure 3. The resulting ground state $S = 15/2$ is in agreement with that determined experimentally. Concerning compound **2**, a fit of the $M = f(HT^{-1})$ curve at 2, 3, and 4 K considering the Hamiltonian in Equation (1) with $g = 2.00$ afforded the parameters $S = 5$, $|D| = 0.49\ cm^{-1}$, and $|E/D| = 0$ ($R = 4.0 \times 10^{-4}$)[21] (Figure SI7 in the Supporting Information). The ground-state spin value determined by this method is in agreement with the $\chi_M T = f(T)$ curve related to **2** (Figure SI8 in the Supporting Information), which reaches a maximum at 18 K with $\chi_M T = 16.0\ cm^3 mol^{-1} K$ ($\chi_M T = 15.0\ cm^3 mol^{-1} K$ for a $S = 5$ ground state assuming $g = 2.00$).

Single-crystal M versus H studies were performed on an array of micro-SQUIDs[24] for complexes **1** and **2**. For complex **1**, the $M = f(H)$ curves show hysteresis loops at low temperatures. The coercive field decreases when the temperature increases (Figure 4, top) and increases when the field-sweeping rate increases at a fixed temperature (Figure SI9 in the Supporting Information). This finding indicates that **1** is a SMM, characterized by a blocking temperature T_b of approximately 0.6 K, above which there is no hysteresis. Nevertheless, the $M = f(H)$ curves related to **1** do not show

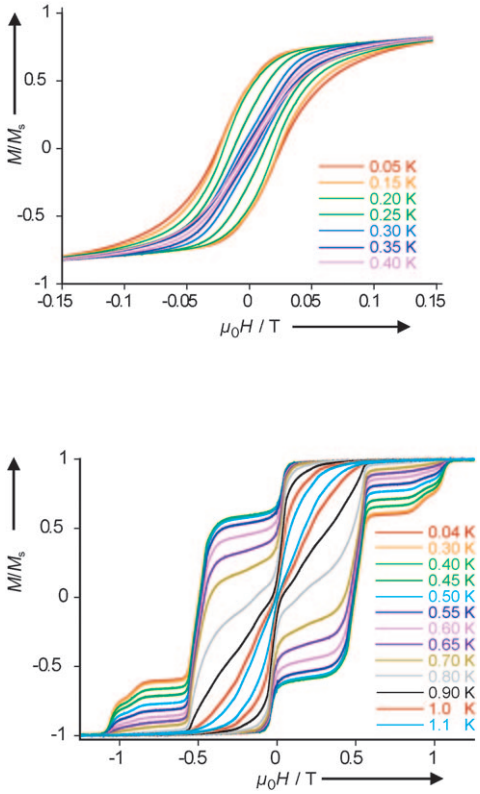

Figure 4. Magnetization versus magnetic field hysteresis loops at the indicated temperature at a sweep rate of 0.035 $T s^{-1}$ for a single crystal of **1** (top) and at a sweep rate of 0.070 $T s^{-1}$ for a single crystal of **2** (bottom). The magnetization is normalized to its saturation value M_s.

the steps characteristic of QTM. This behavior is typical for SMMs with small anisotropy, which are more susceptible to step-broadening effects associated with low-lying excited states, intermolecular interactions, and distributions of local environments. For **2**, the $M = f(H)$ curve is characterized at low temperatures ($T_b \approx 1.2$ K) by stepped hysteresis, with steps at periodic values of the applied field (Figure 4, bottom), demonstrating the occurrence of QTM in **2** whenever the applied field brings energy levels in coincidence. After applying a negative saturation field, the first step occurs at about −0.03 T, establishing very small antiferromagnetic interactions between molecules. Similar to compound **1**, the coercive field decreases for increasing temperature (Figure 4, bottom) and increases for a faster field-sweeping rate (Figure SI10 in the Supporting Information), thereby confirming the SMM behavior of **2**. The field separation between successive steps is given by $\Delta H = |D|(g\mu_B)^{-1}$.[25] This relation leads to $|D| = 0.47\ cm^{-1}$, in excellent agreement with the value determined by the fit of $M = f(H)$ in the 2–4 K temperature range. Note the presence of a small step at about 0.9 T that is probably due to spin–spin cross-relaxation.[26] A plot of the relaxation time versus $1/T$ is shown in Figure SI11 in the Supporting Information. The fit of the thermally activated region ($T > 0.3$ K) gave $\tau_0 = 2.0 \times 10^{-6}\ s^{-1}$ and $U_{eff} = 11.6\ cm^{-1}$. This value of U_{eff} is in excellent agreement with the calculated $U = |D|\ S^2 = 11.75\ cm^{-1}$.

In conclusion, we have shown that it is possible to synthesize high-nuclearity POM clusters incorporating paramagnetic heteroatoms and possessing ground states with large spin multiplicity. The extension of this family of POM compounds to other 3d centers is currently under study. The iron POMs presented herein exhibit SMM behavior, and the hexanuclear Fe^{III} complex shows clear QTM effects. The reported compounds are stable in solution for a wide range of pH values, allowing their grafting on carbon nanotubes. The magnetic and electrocatalytic properties of these devices will be reported soon.

Experimental Section

1 and **2**: $Na_2WO_4{\cdot}2H_2O$ (0.800 g, 2.43 mmol), $FeCl_3{\cdot}6H_2O$ (0.340 g, 1.26 mmol), and tetramethylammonium bromide (0.400 g, 2.6 mmol) in water (5 mL) were stirred, and the pH value was adjusted to 7.0 by addition of 2 M aqueous NaOH. The obtained mixture was sealed in a 23 mL teflon-lined stainless steel reactor, heated to 160 °C over one hour, maintained at this temperature for 44 h, and then cooled down to room temperature over a period of 44 h. The resulting mixture was filtered and the filtrate left to slowly evaporate. After two days, large orange crystals of **1** were filtered off (70 mg, 9 % yield based on W). Elemental analysis calcd (%) for $Na_{14}Fe_9W_{24}O_{146}C_{12}H_{140}N_3$: W 55.8, Fe 6.36, Na 4.07, C 1.82, H 1.79, N 0.53; found: W 55.0, Fe 5.97, Na 3.25, C 1.72, H 1.67, N 0.48. Crystal data ($T = 100$ K) for **1**: triclinic, $P\bar{1}$, $a = 13.4678(11)$, $b = 15.1320(12)$, $c = 15.3939(12)$ Å, $\alpha = 111.082(4)$, $\beta = 98.785(4)$, $\gamma = 104.592(3)°$, $V = 2728.0(4)$ Å^3, $Z = 1$, $\rho = 3.661\ g\,cm^{-3}$, $\mu = 19.814\ mm^{-1}$, $F(000) = 2740$, $GOF = 1.177$. A total of 115694 reflections were collected, 15824 of which were unique ($R_{int} = 0.0363$). R_1 (wR_2) = 0.0306 (0.0921) for 671 parameters. Further evaporation of the filtrate led after several days to small yellow crystals of **2** (100 mg, 12 % yield based on W). Elemental analysis calcd (%) for $Na_6Fe_6W_{18}O_{115}C_{16}H_{142}N_4$: W 55.0, Fe 5.57, Na 2.29, C 3.20, H 2.38, N 0.93; found: W 55.7, Fe 5.49, Na 3.03, C 3.11, H 2.07, N 0.86. Crystal data ($T = 100$ K) for **2**: monoclinic, $P2_1/n$, $a = 22.444(6)$, $b = 25.517(6)$, $c = 23.629(6)$ Å, $\beta = 100.079(13)°$, $V = 13323(6$ Å^3, $Z = 4$, $\rho = 3.990\ g\,cm^{-3}$, $\mu = 21.748\ mm^{-1}$, $F(000) = 14516$, $GOF = 1.169$. A total of 264730 reflections were collected, 38339 of which were unique ($R_{int} = 0.0551$). R_1 (wR_2) = 0.0588 (0.1454) for 1706 parameters. CCDC 712880 (**1**) and 712879 (**2**) contain the supplementary crystallographic data for this paper. These data can be obtained free of charge from The Cambridge Crystallographic Data Centre via www.ccdc.cam.ac.uk/data_request/cif.

Received: January 8, 2009
Published online: March 25, 2009

Keywords: electrochemistry · iron · polyoxometalates · single-molecule magnets

[1] a) D. Gatteschi, R. Sessoli, *Angew. Chem.* **2003**, *115*, 278 – 309; *Angew. Chem. Int. Ed.* **2003**, *42*, 268 – 297; b) G. Christou, *Polyhedron* **2005**, *24*, 2065 – 2075; c) E. K. Brechin, *Chem. Commun.* **2005**, 5141 – 5153.

[2] W. Wernsdorfer, S. Badhuri, C. Boskovic, G. Christou, D. N. Hendrickson, *Phys. Rev. B* **2002**, *65*, 180403.

[3] a) R. Giraud, W. Wernsdorfer, A. M. Tkachuk, D. Mailly, B. Barbara, *Phys. Rev. Lett.* **2001**, *87*, 057203; b) N. Ishikawa, M. Sugita, T. Ishikawa, S. Koshihara, Y. Kaizu, *J. Am. Chem. Soc.* **2003**, *125*, 8694 – 8695; c) N. Ishikawa, M Sugita, W. Wernsdorfer, *Angew. Chem.* **2005**, *117*, 2991 – 2995; *Angew. Chem. Int. Ed.* **2005**, *44*, 2931 – 2935.

[4] C. Ritchie, A. Ferguson, H. Nojiri, H. N. Miras, Y.-F. Song, D.-L. Long, E. Burkholder, M. Murrie, P. Kögerler, E. K. Brechin, L. Cronin, *Angew. Chem.* **2008**, *120*, 5691 – 5694; *Angew. Chem. Int. Ed.* **2008**, *47*, 5609 – 5612.

[5] M. A. AlDamen, J. M. Clemente-Juan, E. Coronado, C. Martí-Castaldo, A. Gaita-Ariño, *J. Am. Chem. Soc.* **2008**, *130*, 8874 – 8875.

[6] C. Pichon, P. Mialane, E. Rivière, G. Blain, A. Dolbecq, J. Marrot, F. Sécheresse, C. Duboc, *Inorg. Chem.* **2007**, *46*, 7710 – 7712.

[7] S.-T. Zheng, D.-Q. Yuan, H.-P. Jia, J. Zhang, G.-Y. Yang, *Chem. Commun.* **2007**, 1858 – 1860.

[8] J. M. Clemente-Juan, E. Coronado, *Coord. Chem. Rev.* **1999**, *193–195*, 361.

[9] J. M. Clemente-Juan, E. Coronado, J. R. Galán-Mascarós, C. J. Gómez-Garcia, *Inorg. Chem.* **1999**, *38*, 55 – 63.

[10] P. Mialane, A. Dolbecq, J. Marrot, E. Rivière, F. Sécheresse, *Angew. Chem.* **2003**, *115*, 3647 – 3650; *Angew. Chem. Int. Ed.* **2003**, *42*, 3523 – 3526.

[11] B. Godin, Y.-G. Chen, J. Vaissermann, L. Ruhlmann, M. Verdaguer, P. Gouzerh, *Angew. Chem.* **2005**, *117*, 3132 – 3135; *Angew. Chem. Int. Ed.* **2005**, *44*, 3072 – 3075.

[12] S. S. Mal, U. Kortz, *Angew. Chem.* **2005**, *117*, 3843 – 3846; *Angew. Chem. Int. Ed.* **2005**, *44*, 3777 – 3780.

[13] a) N. Casañ-Pastor, P. Gomez-Romero, G. B. Jameson, L. C. W. Baker, *J. Am. Chem. Soc.* **1991**, *113*, 5658 – 5663; b) C. J. Gómez-Garcia, C. Giménez-Saiz, S. Triki, E. Coronado, P. Le Magueres, L. Ouahab, L. Ducasse, C. Sourisseau, P. Delhaes, *Inorg. Chem.* **1995**, *34*, 4139 – 4151.

[14] J. Server-Carrió, J. Bas-Serra, M. E. González-Nùñez, A. García-Gastaldi, G. B. Jameson, L. C. W. Baker, R. Acerete, *J. Am. Chem. Soc.* **1999**, *121*, 977 – 984.

[15] H. Andres, J. M. Clemente-Juan, R. Basler, H. U. Güdel, J. J. Borrás-Almenar, A Gaita, E. Coronado, H. Büttner, S. Janssen, *Inorg. Chem.* **2001**, *40*, 1943 – 1950.

[16] a) J. Wang, P. Ma, Y. Shen, J. Niu, *Cryst. Growth Des.* **2007**, *7*, 603 – 605; b) A. Dolbecq, J.-D. Compain, P. Mialane, J. Marrot, E. Rivière, F. Sécheresse, *Inorg. Chem.* **2008**, *47*, 3371 – 3378;

c) E. M. Limanski, M. Piepenbrink, E. Droste, K. Burgemeister, B. Krebs, *J. Cluster Sci.* **2002**, *13*, 369 – 379.
[17] R. Blessing, *Acta Crystallogr. Sect. A* **1995**, *51*, 33.
[18] a) I. M. Mbomekallé, B. Keita, M. Nierlich, U. Kortz, P. Berthet, L. Nadjo, *Inorg. Chem.* **2003**, *42*, 5143 – 5152; b) J. M. Clemente-Juan, E. Coronado, A. Forment-Aliaga, J. R. Galàn-Mascarós, C. Giménez-Saiz, C. J. Gómez-Garcia, *Inorg. Chem.* **2004**, *43*, 2689 – 2694.
[19] D. Barats, G. Leitus, R. Popovitz-Biro, L. J. W. Shimon, R. Neumann, *Angew. Chem.* **2008**, *120*, 10056 – 10060; *Angew. Chem. Int. Ed.* **2008**, *47*, 9908 – 9912.
[20] a) I. M. Mbomekallé, B. Keita, L. Nadjo, P. Berthet, K. I. Hardcastle, C. L. Hill, T. M. Anderson, *Inorg. Chem.* **2003**, *42*, 1163 – 1169; b) B. Keita, I. M. Mbomekallé, Y. W. Lu, L. Nadjo, P. Berthet, T. M. Anderson, C. L. Hill, *Eur. J. Inorg. Chem.* **2004**, 3462 – 3475; c) B. Keita, L. Nadjo, *Electrochemistry of Polyoxometalates, Encyclopedia of Electrochemistry, Vol. 7* (Eds.: A. J. Bard, M. Stratmann), Wiley-VCH, Weinheim, **2006**, pp. 607 – 700.
[21] $R = [\Sigma(M_{calcd} - M_{obs})^2/\Sigma(M_{obs})^2]$.
[22] a) H. Weihe, H. U. Güdel, *J. Am. Chem. Soc.* **1997**, *119*, 6539 – 6543; b) S. M. Gorun, S. J. Lippard, *Inorg. Chem.* **1991**, *30*, 1625 – 1630; c) R. Bagai, M. R. Daniels, K. A. Abboud, G. Christou, *Inorg. Chem.* **2008**, *47*, 3318 – 3327.
[23] C. Pichon, A. Dolbecq, P. Mialane, J. Marrot, E. Rivière, M. Goral, M. Zynek, T. McCormac, S. Borshch, E. Zueva, F. Sécheresse, *Chem. Eur. J.* **2008**, *14*, 3189 – 3199.
[24] W. Wernsdorfer, *Adv. Chem. Phys.* **2001**, *118*, 99 – 189.
[25] T. C. Stamatatos, D. Foguet-Albiol, S.-C. Lee, C. C. Stoumpos, C. P. Raptopoulou, A. Terzis, W. Wernsdorfer, S. O. Hill, S. P. Perlepes, G. Christou, *J. Am. Chem. Soc.* **2007**, *129*, 9484 – 9499.
[26] W. Wernsdorfer, S. Badhuri, R. Tiron, D. N. Hendrickson, G. Christou, *Phys. Rev. Lett.* **2002**, *89*, 197201.

